

Part I: Binary Oxide Catalysts of Alumina–Rare Earth Oxides

Janakiamma Jayasree and Cadavallore S. Narayanan*

Regional Research Laboratory (CSIR), Thiruvananthapuram, Kerala-695019, India

(Received January 7, 1994)

Binary oxides of alumina with rare earths like europium, samarium, praseodymium, neodymium, and yttrium were prepared by coprecipitation from corresponding nitrates. The composition, thermal stability, and surface properties of the catalysts were determined using XRD, TGA, XPS, and MAS ^{27}Al NMR. Surface area and pore size of the catalysts were determined by BET and mercury porosimetry. The catalysts were found to be amorphous and aluminium atom showed tetrahedral and octahedral coordination in its lattice. Catalysts showed weak to moderate acidity and basicity.

Surface and catalytic properties of binary oxides of aluminium with various other oxides have been investigated by a number of workers.^{1–4)} Rare earth exchanged zeolites are widely used as cracking catalysts in petrochemical industries. But little attention has been paid for the study of binary oxides of aluminium and rare earths. Hence the present work was initiated to study the surface and physicochemical properties of alumina–rare earth oxides.

Experimental

Materials: $\text{Al}(\text{NO}_3)_3 \cdot 9\text{H}_2\text{O}$ used for the preparation of alumina was obtained from E. Merck (India) Ltd. Rare earth oxides used were of 99.9% purity supplied by Indian Rare Earths Ltd. All solvents used were AR grade and distilled over sodium.

Preparation of Catalysts. **Preparation of Al_2O_3 – Y_2O_3 (1:1):** $\text{Al}(\text{NO}_3)_3 \cdot 9\text{H}_2\text{O}$ (55.5 g) was dissolved in water (400 ml). Y_2O_3 (7.5 g) was dissolved in minimum amount of 1:1 HNO_3 –water solution. These solutions were mixed together and 15 g of NH_4NO_3 added. Ammonia solution (25%) was added to this mixture to a final pH 10. The precipitate formed was aged for 20 h, filtered and washed with distilled water and dried at 130 °C for 24 h. The hydroxides were calcined in air at 400 °C for 5 h. Al_2O_3 – Sm_2O_3 , Al_2O_3 – Pr_6O_{11} , Al_2O_3 – Nd_2O_3 , and Al_2O_3 – Eu_2O_3 were prepared by following the same procedure for Al_2O_3 – Y_2O_3 .

Chemical Estimation: The composition of binary oxide was determined by precipitating the rare earth as oxalate.⁵⁾ The oxalate is converted to oxide by ignition. From the weight of rare earth oxide, the weight of alumina in the mixture was determined.

X-Ray Analysis and TGA: X-Ray diffraction pattern was recorded on a Phillips 1710 (Holland) diffractometer. Radiation source was $\text{Cu K}\alpha$. Samples scanned between 20–60 °C. TGA of the hydroxides were carried out in a stream of air from ambient to 900 °C, at the rate of

20 °C min^{-1} . TGA was done on a 951 thermogravimetric analyser (Dupont Instruments).

Surface Area and Pore Volume: Surface areas of the catalysts were measured by BET method of N_2 adsorption at –196 °C on a Quantasorb Jr. S. A. analyser. Pore volume distributions were determined by mercury intrusion technique on Autoscan 60 porosimeter.

Acidity and Basicity Measurement: Acidity of the catalysts were determined by Benesis' method⁶⁾ using the following Hammett indicators. Neutral red (+6.8), α -naphthyl red (+4), methyl yellow (+3.3), (4-phenyl azo) diphenyl amine (+1.5), dicinnamal acetone (–3), benzal acetophenone (–5.6), and anthraquinone (–8.2). Acid density distribution of catalysts are determined by titrating benzene solutions of *n*-butyl amine with catalyst samples in benzene. Basicity of catalysts were determined by indicators like 2,4,6-trinitroaniline (12.2), 2,4-dinitroaniline (15.0), 4-nitroaniline (18.4), and 4-chloro aniline (26.5) by method of Yoneda et al.⁷⁾ Basic strength distribution was determined by titrating catalyst in cyclohexane with benzoic acid.

X-Ray Photoelectron Spectroscopy: XPS measurements were carried out on an ESCA-3MKII electron spectrometer (V.G. Scientific, U.K.). Photoelectrons were excited using $\text{Al K}\alpha$ (1486.6 eV) radiation. The electron energy analyser was operated in the constant at analyser energy mode at a pass energy of 20 eV. The spectrometer was calibrated to give the Au 4f-7/2 line at 84 eV. Binding energy values were measured with an accuracy of ± 0.2 eV.

MAS ^{27}Al NMR: MAS ^{27}Al NMR of the samples were taken on Bruker MSL 300 (frequency 78.2). Reference used was NaY zeolite at 62.8 ppm. Sweep width 250 kHz. Pulse length 1 micro second, relaxation delay 500 ms.

Results and Discussion

Binary oxide catalysts were prepared by coprecipitation as hydroxides from nitrate solution. NH_3 solution is added in one lot with efficient stirring resulting in the initial precipitation of rare earth hydroxides. Gravimet-

ric estimation of catalyst does not show much variation in the composition from theoretical values showing complete precipitation of aluminium and rare earths. Pure aluminium hydroxide precipitated and calcined at 400 °C showed highly amorphous nature probably due to residual microporosities (Fig. 1). Hydrated single oxides like Eu_2O_3 , Sm_2O_3 , and Pr_6O_{11} showed diffraction lines showing its partial crystalline nature. In Fig. 2 the XRD patterns of binary oxides are given and it illustrates its amorphous nature.

As evident from Fig. 3 rare earth oxides show a general tendency to bring down the final decomposition temperature to about 550 °C. Pr_6O_{11} , Sm_2O_3 , and Eu_2O_3 influence the major decomposition peak such that the decomposition takes place between 286 and 296 °C suggesting a low extent of free OH groups in these oxides. Among these three binary oxides $\text{Al}_2\text{O}_3\text{--Eu}_2\text{O}_3$

showed a sharp decomposition showing major water removal. $\text{Al}_2\text{O}_3\text{--Nd}_2\text{O}_3$ showed an isolate decomposition at 280–290 °C range showing retention of free OH group in the hydroxide gel which is further evidenced by surface area measurements. The surface area and chemical composition values of different binary oxides are given in Table 1. Though the method of precipitation of catalysts were same, the surface area of $\text{Al}_2\text{O}_3\text{--Pr}_6\text{O}_{11}$ was found to be low which may be due to agglomeration during precipitation. Except $\text{Al}_2\text{O}_3\text{--Nd}_2\text{O}_3$ surface area values are in tune with thermal decomposition data. The high surface area of $\text{Al}_2\text{O}_3\text{--Nd}_2\text{O}_3$ system is due to slow decomposition of its hydroxide.

Pore number (γ) versus radius of various binary oxide catalysts are depicted in Fig. 4. All five binary oxides show different patterns in pore size distribution. Among

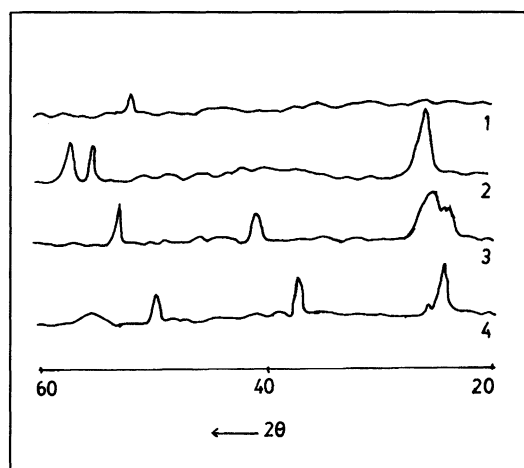


Fig. 1. XRD spectra of single oxide. 1. Al_2O_3 ; 2. Sm_2O_3 ; 3. Eu_2O_3 ; 4. Pr_6O_{11} .

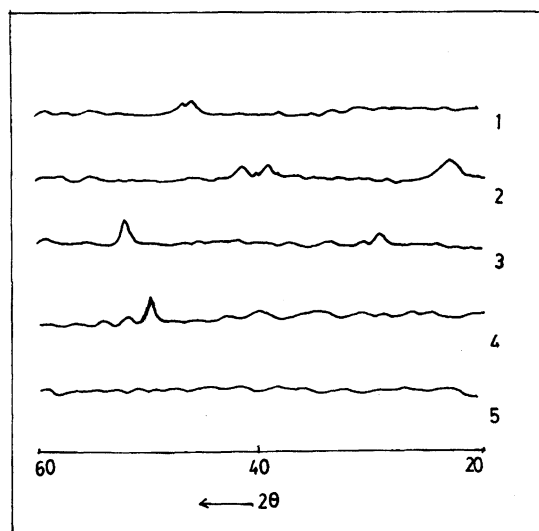


Fig. 2. XRD spectra of binary oxides. 1. $\text{Al}_2\text{O}_3\text{--Y}_2\text{O}_3$; 2. $\text{Al}_2\text{O}_3\text{--Sm}_2\text{O}_3$; 3. $\text{Al}_2\text{O}_3\text{--Pr}_6\text{O}_{11}$; 4. $\text{Al}_2\text{O}_3\text{--Nd}_2\text{O}_3$; 5. $\text{Al}_2\text{O}_3\text{--Eu}_2\text{O}_3$.

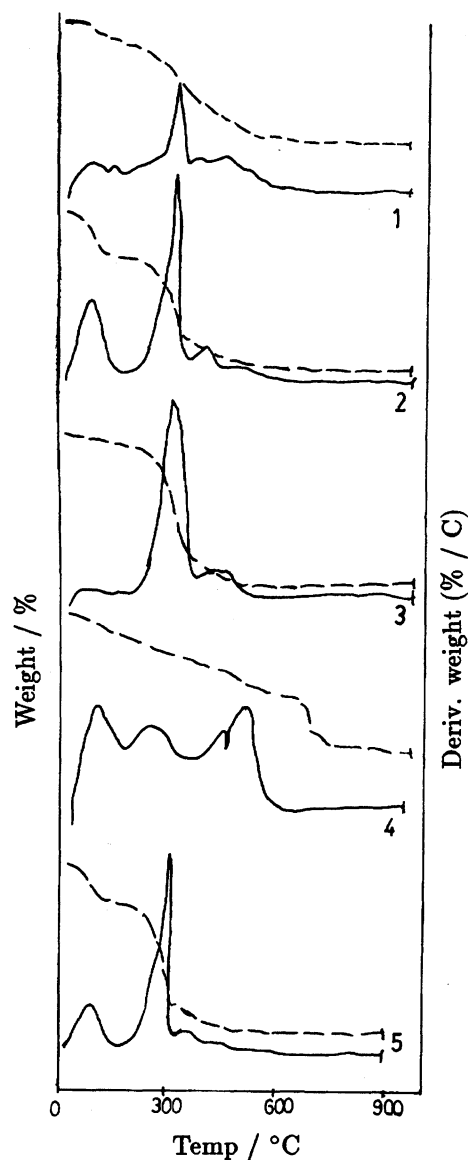


Fig. 3. TGA (....) and DTG (—) curves of catalysts. 1. $\text{Al}_2\text{O}_3\text{--Y}_2\text{O}_3$; 2. $\text{Al}_2\text{O}_3\text{--Sm}_2\text{O}_3$; 3. $\text{Al}_2\text{O}_3\text{--Pr}_6\text{O}_{11}$; 4. $\text{Al}_2\text{O}_3\text{--Nd}_2\text{O}_3$; 5. $\text{Al}_2\text{O}_3\text{--Eu}_2\text{O}_3$.

the catalysts $\text{Al}_2\text{O}_3\text{-Y}_2\text{O}_3$ showed a wide distribution of pore from 20 Å to 1000 Å while $\text{Al}_2\text{O}_3\text{-Pr}_6\text{O}_{11}$ had a narrow distribution of 20–25 Å. The pore surface area values of different catalysts calculated by mercury porosimetry are given in Table 1. The small surface area values in mercury porosimetry indicates a bimodal pore size distribution in these oxides.⁸⁾

Acidic and Basic Properties: The single oxide catalysts of rare earth showed acidic sites ranging

Table 1. Physicochemical Characteristics of Catalysts

Catalyst 1 : 1	Chemical estimation value w/w	Surface area (BET) $\text{m}^2 \text{g}^{-1}$	Surface area mercury instruction $\text{cm}^2 \text{g}^{-1}$
$\text{Al}_2\text{O}_3\text{-Y}_2\text{O}_3$	1 : 0.952	101.825	30.641
$\text{Al}_2\text{O}_3\text{-Sm}_2\text{O}_3$	1 : 0.923	97.351	37.877
$\text{Al}_2\text{O}_3\text{-Pr}_6\text{O}_{11}$	1 : 0.934	42.517	4.431
$\text{Al}_2\text{O}_3\text{-Eu}_2\text{O}_3$	1 : 0.952	101.250	28.398
$\text{Al}_2\text{O}_3\text{-Nd}_2\text{O}_3$	1 : 0.943	121.507	21.793

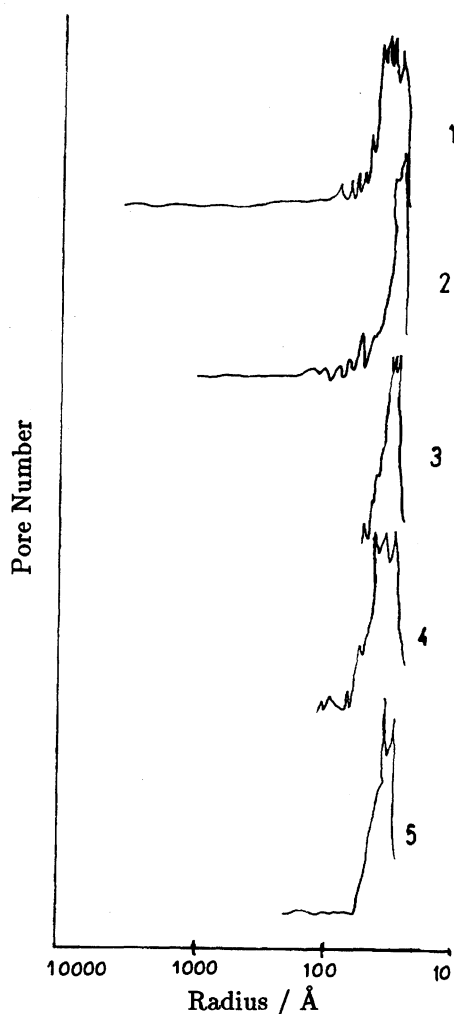


Fig. 4. Pore number (r) versus radius of various catalysts. 1. $\text{Al}_2\text{O}_3\text{-Y}_2\text{O}_3$; 2. $\text{Al}_2\text{O}_3\text{-Sm}_2\text{O}_3$; 3. $\text{Al}_2\text{O}_3\text{-Pr}_6\text{O}_{11}$; 4. $\text{Al}_2\text{O}_3\text{-Nd}_2\text{O}_3$; 5. $\text{Al}_2\text{O}_3\text{-Eu}_2\text{O}_3$.

in between +3.3 to +1.5. Al_2O_3 showed acid strength in between $H_0 \leq +1.5$ to -5.6 . Binary oxides showed an acidity range from $H_0 \leq -5.6$ to -8.2 showing that there is increase in acid strength of binary oxides when compared to single oxides. This can be accounted by the formation of more strained sites on catalyst surface during coprecipitation and calcination.

The amount of acid sites at different Hammet acid strengths on unit surface area for four catalysts are given in Fig. 5. The acid sites on $\text{Al}_2\text{O}_3\text{-Pr}_6\text{O}_{11}$ could not be estimated due to the dull green color of the catalyst. At $H_0 \leq +6.8$, Al_2O_3 had a maximum acid amount of $0.114 \text{ mmol m}^{-2}$ and $\text{Al}_2\text{O}_3\text{-Nd}_2\text{O}_3$ had $0.107 \text{ mmol m}^{-2}$. The least acid amount was observed for $\text{Al}_2\text{O}_3\text{-Y}_2\text{O}_3$. At $H \leq +4$, these binary oxide catalysts followed the same trend of acidity. At medium acid strength of $H_0 \leq +3.3$ and $+1.5$, $\text{Al}_2\text{O}_3\text{-Eu}_2\text{O}_3$ showed highest acid amount of 0.035 and $0.038 \text{ mmol m}^{-2}$. At medium acid strength, $\text{Al}_2\text{O}_3\text{-Sm}_2\text{O}_3$ was found to have more acid amount than $\text{Al}_2\text{O}_3\text{-Nd}_2\text{O}_3$. At higher acid sites $H_0 \leq -3$, $\text{Al}_2\text{O}_3\text{-Eu}_2\text{O}_3$ showed maximum acidity followed by $\text{Al}_2\text{O}_3\text{-Sm}_2\text{O}_3$. Thus from acidity values in Fig. 5 it is clear that the catalysts have weak to moderate acidity.

All the four binary oxide catalysts showed basicity values in the PkbH range 12.2 to 15.0. The basic strength of different catalysts are given in Table 2. $\text{Al}_2\text{O}_3\text{-Nd}_2\text{O}_3$ showed highest total basicity. $\text{Al}_2\text{O}_3\text{-Eu}_2\text{O}_3$ has got more basic amount of $0.286 \text{ mmol m}^{-2}$ at PkbH 15. $\text{Al}_2\text{O}_3\text{-Nd}_2\text{O}_3$ has got basic amount of $0.255 \text{ mmol m}^{-2}$ at this PkbH value. $\text{Al}_2\text{O}_3\text{-Sm}_2\text{O}_3$ has intermediate basicity and

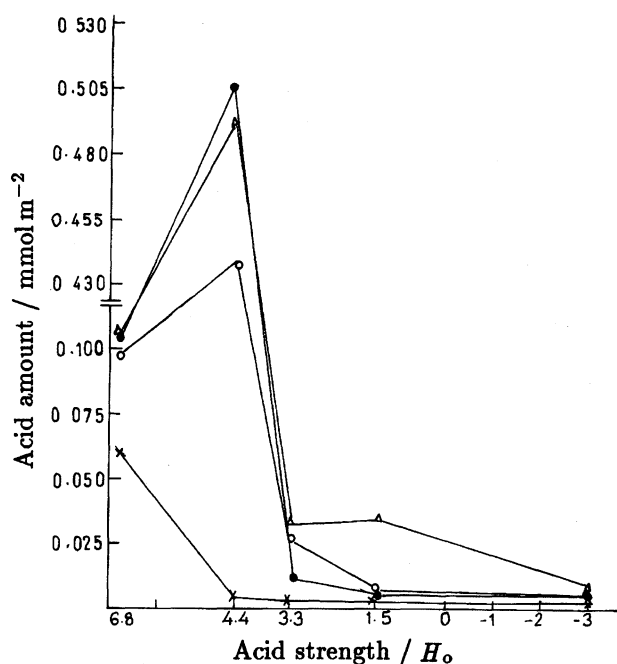


Fig. 5. Acid amount at different acid strengths of catalysts. -x- $\text{Al}_2\text{O}_3\text{-Y}_2\text{O}_3$; -Δ- $\text{Al}_2\text{O}_3\text{-Eu}_2\text{O}_3$; -●- $\text{Al}_2\text{O}_3\text{-Nd}_2\text{O}_3$; -○- $\text{Al}_2\text{O}_3\text{-Sm}_2\text{O}_3$.

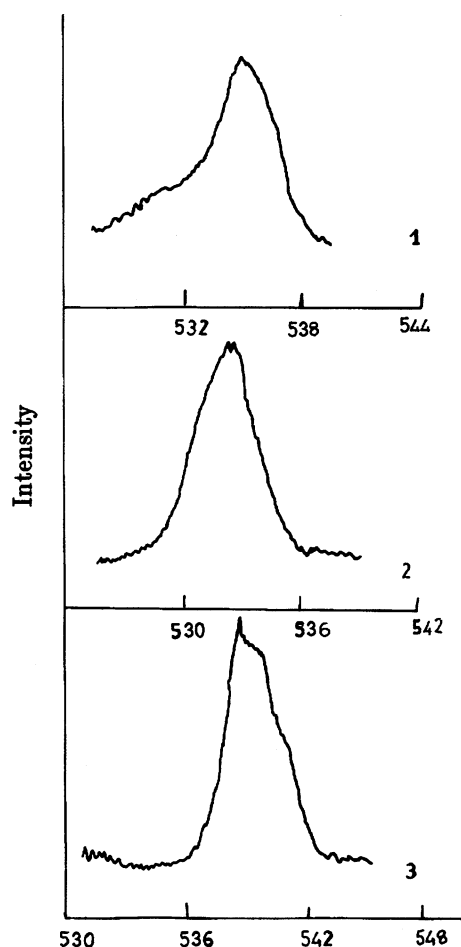
$\text{Al}_2\text{O}_3\text{-Y}_2\text{O}_3$ has the least value.

Basic strength of mixed oxides can be obtained from XPS analysis, since binding energy values obtained from XPS is indicative of site strength. The OIS binding energy is a measure for electron pair donating ability of the oxides.⁹⁾ The order of basic strength obtained from XPS data is $\text{Al}_2\text{O}_3\text{-Nd}_2\text{O}_3 > \text{Al}_2\text{O}_3\text{-Pr}_6\text{O}_{11} > \text{Al}_2\text{O}_3\text{-Eu}_2\text{O}_3$. The difference in measured binding energy in Fig. 6 is very small. The binary oxides show marked difference in basicity at different PkBH values.

Single oxides of rare earths prepared under similar precipitation conditions did not show any sites at all,

Table 2. Basic Strength Distribution of Different Catalysts

Catalyst	Basic amount in mmol m^{-2} in PkBH range		Total basicity mmol m^{-2}
	12.2	15	
$\text{Al}_2\text{O}_3\text{-Y}_2\text{O}_3$	0.023	0.045	0.068
$\text{Al}_2\text{O}_3\text{-Sm}_2\text{O}_3$	0.123	0.131	0.254
$\text{Al}_2\text{O}_3\text{-Eu}_2\text{O}_3$	0.059	0.286	0.345
$\text{Al}_2\text{O}_3\text{-Nd}_2\text{O}_3$	0.124	0.255	0.379



B. E.

Fig. 6. XPS spectra of various catalysts. 1. $\text{Al}_2\text{O}_3\text{-Nd}_2\text{O}_3$; 2. $\text{Al}_2\text{O}_3\text{-Pr}_6\text{O}_{11}$; 3. $\text{Al}_2\text{O}_3\text{-Eu}_2\text{O}_3$.

but Al_2O_3 showed weak basicity. There is definite increase in basic strength of mixed oxides indicating generation of basic sites on the surface.

Even though there is difference in the pH for the precipitation of rare earths and alumina the absence of Al_2O_3 crystallites and rare earth oxide crystallites indicated by XRD shows that the binary metal oxides are not mechanical mixtures but consists of new complex oxides. This could be in the form of metal-o-metal type of linkages.

All catalysts used in the study produced two chemical shifts in ^{27}Al NMR spectrum (Fig. 7). One around 60 ppm and other around zero to 10 ppm. The former shift has been attributed for Al atom in tetrahedral coordination whereas the latter for octahedral coordination of aluminium. Akitt et al. have shown that the band around 10 ppm can be accounted for the presence of Al^{3+} ion.¹⁰⁾ This Al^{3+} ion can be the sites on catalyst surface giving Lewis as well as Brönsted acidity to catalyst.

Conclusion

The binary oxide catalysts prepared by coprecipitation showed wide distribution of pore size and surface area which is inexplicable from their decomposition pattern. The catalysts showed more acidity and basicity than the single oxides. The activity of the catalysts were studied in the transformation of terpenyl oxiranes like α and β -pinene oxides. This part of the study is detailed in Part II publication of the series.

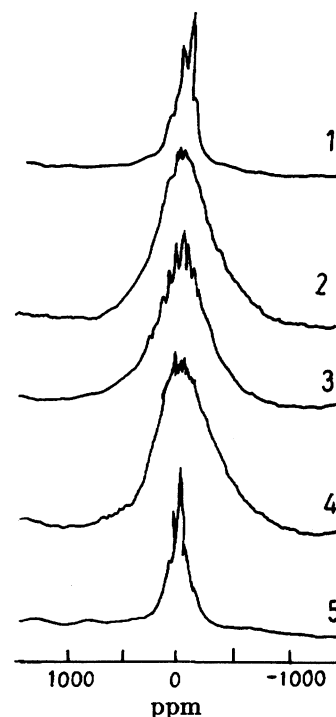


Fig. 7. MAS ^{27}Al NMR spectra of catalysts. 1. $\text{Al}_2\text{O}_3\text{-Y}_2\text{O}_3$; 2. $\text{Al}_2\text{O}_3\text{-Pr}_6\text{O}_{11}$; 3. $\text{Al}_2\text{O}_3\text{-Eu}_2\text{O}_3$; 4. $\text{Al}_2\text{O}_3\text{-Nd}_2\text{O}_3$; 5. $\text{Al}_2\text{O}_3\text{-Sm}_2\text{O}_3$.

The author J. J. is grateful to CSIR (India) for a research fellowship.

References

- 1) E. Rodenas, T. Yamaguchi, H. Hattori, and K. Tanabe, *J. Catal.*, **69**, 434 (1981).
 - 2) K. Shibata, T. Kiyoura, J. Kitagawa, T. Sumiyoshi, and K. Tanabe, *Bull. Chem. Soc. Jpn.*, **46**, 2985 (1973).
 - 3) K. Tanabe, K. Shimizu, H. Hattori, and K. Shimazu, *J. Catal.*, **57**, 35 (1979).
 - 4) H. Kawakami, and S. Yoshida, *J. Chem. Soc., Faraday Trans. 2*, **81**, 1117 (1985).
 - 5) M. M. Woyski, and R. L. Haris, "Treatise on Analytical Chemistry," Part II, Analytical Chemistry of the Elements, Vol. 8, p.34.
 - 6) H. A. Benesi, *J. Phys. Chem.*, **61**, 970 (1957).
 - 7) J. I. Take, N. Kikuchi, and Y. Yoneda, *J. Catal.*, **21**, 164 (1971).
 - 8) T. Huang, A. White, A. Walpole, and D. L. Trimm, *Appl. Catal.*, **57**, 177 (1989).
 - 9) H. Vinek, H. Noller, M. Ebel, and K. Schwarz, *J. Chem. Soc., Faraday Trans. 1*, **1977**, 734.
 - 10) J. Akitt and A. Farthing, *J. Chem. Soc., Dalton Trans.*, **7**, 1606 (1981).
-